

Chapter 14

Experimental Investigation of Free-Field Implosion of Filament Wound Composite Tubes

M. Pinto and A. Shukla

Abstract The mechanisms and energies associated with the hydrostatic implosion of composite cylinders are investigated experimentally and numerically. Experiments are conducted in a large pressure vessel, designed as to provide an adequate reflection-free window to best capture pressure waves resulting from the collapse. Both glass-fiber/polyester and carbon-fiber/epoxy filament wound thin-walled ($R/t > 15$) tubes are tested with varying L/D ratios to explore the effect of geometry on the collapse pressure and mechanics of the collapse. 3D Digital Image Correlation (DIC) is used to capture the full-field displacements and strains during the implosion event, and dynamic pressure transducers are employed to measure the pressure pulse generated by the collapse. Computational models are developed to verify and better understand key mechanisms of failure during hydrostatic buckling.

Keywords Composite cylinders • Hydrostatic implosion • Filament winding • Digital image correlation • High-speed photography

14.1 Introduction

The use of composites has attracted attention in underwater marine applications due to the array of advantages offered by these materials. Composite materials offer alternatives with reduced weight, improved corrosion resistance, and for submerged structures, greater potential operating depths. In addition, these materials provide improved stealth qualities by having very low thermal, acoustic, and magnetic signatures, increasing their appeal for military applications. For these reasons, the presence of composite materials in marine industries is increasing, and they are currently used in several naval applications, such as sonar domes, masts, and hull sheathings [1]. One of the biggest obstacles to widespread adaptation of composite materials is a lack of complete understanding and simple design rules for these materials, especially under extreme loading conditions [1]. For this reason, this work looks to expand the current knowledge of composite behavior by examining the problem of implosion.

The implosion of a submerged structure occurs when external pressure reaches a critical value, causing an instability in the structure and resulting in a rapid and often catastrophic collapse. During this collapse, the boundaries of the volume and the surrounding fluid are accelerated to high velocities and stop suddenly once the collapse is completed. This abrupt change in momentum releases a pressure wave into the surrounding fluid, which can have the potential to damage nearby structures [2, 3]. For this reason, the implosion problem has gained much attention in recent decades. The implosion of glass spheres has been studied by several authors who characterized the pressure pulse emitted during collapse as well as its potential for damage to nearby structures [4–6]. The implosion of aluminum cylinders has also been studied in recent work. Turner identified key stages of the implosion event in relation to the local pressure about the collapsing structure [7]. Farhat et al. studied the implosion of aluminum cylinders with varying L/D ratios to produce both mode 2 and mode 4 failures [8].

M. Pinto • A. Shukla (✉)
Dynamics Photomechanics Laboratory, Department of Mechanical, Industrial and Systems Engineering,
University of Rhode Island, Kingston, RI 02881, USA
e-mail: mpinto@umassd.edu; shuklaa@egr.uri.edu

In this work, the authors were able to observe the differences in the emitted pressure pulse as well as the collapse progression due to the change in buckling mode. In both works by Turner and Farhat, robust fluid–structure computational models were developed which correlated quite well with experimental data.

Though several analytical treatments exist on the subject, the implosion of composite cylinders under hydrostatic loading has also been experimentally studied in a few previous publications. Moon et al. examined implosion of filament-wound carbon/epoxy composite tubes with different winding angles both experimentally and computationally to determine collapse pressures and modes [9]. Both Ross and Smith performed experiments on carbon/E-glass tubes to determine critical buckling pressure, buckling modes, and create design tables for these structures [10, 11]. Hernández-Moreno et al. tested filament-wound glass/epoxy composite tubes with a winding angle of 55° to examine effects of winding pattern on the collapse pressure [12]. Hur et al. examined the buckling modes, loads, and ply failure of carbon/epoxy tape layup tubes both experimentally and computationally [13]. Yang et al. developed an analytic model for critical buckling pressure based on anisotropic laminate theory and performed experiments on E-glass/epoxy tubes to test predictions [14]. However, in none of these studies was the pressure pulse from the collapse measured, nor were high speed images of the collapse event captured. This study addresses the current gap in knowledge by examining the pressure pulses emitted in collapse of filament wound composite tubes and capturing full-field displacements during the implosion event along with a high-speed photographic record of the failure process.

14.2 Materials

The impodable volumes in this study are carbon/epoxy and glass/polyester (PE) filament wound composite tubes. The carbon/epoxy tubes consist of seven layers of unidirectional carbon fabric reinforcement arranged in a $[\pm 15/0/\pm 45/\pm 15]$ layup with a 60.3 mm inner diameter and 305 mm length. These cylinders are manufactured by Rock West Composites (West Jordan, UT) with a nominal wall thickness of 1.63 mm and are thoroughly sanded on the exterior surface for excellent finish and tolerances. The glass/PE tubes consist of five layers of unidirectional E-glass fabric reinforcement arranged in a $[\pm 55/\pm 55/0]$ layup with a 57.2 mm inner diameter and 406 mm length. These cylinders are manufactured by Nor'Easter Yachts (Milford, CT) with a nominal wall thickness of 2 mm. The dimensions are selected as to provide specimens with a relatively low expected collapse pressure, and a high R/t ratio so that thin-wall assumptions may be utilized.

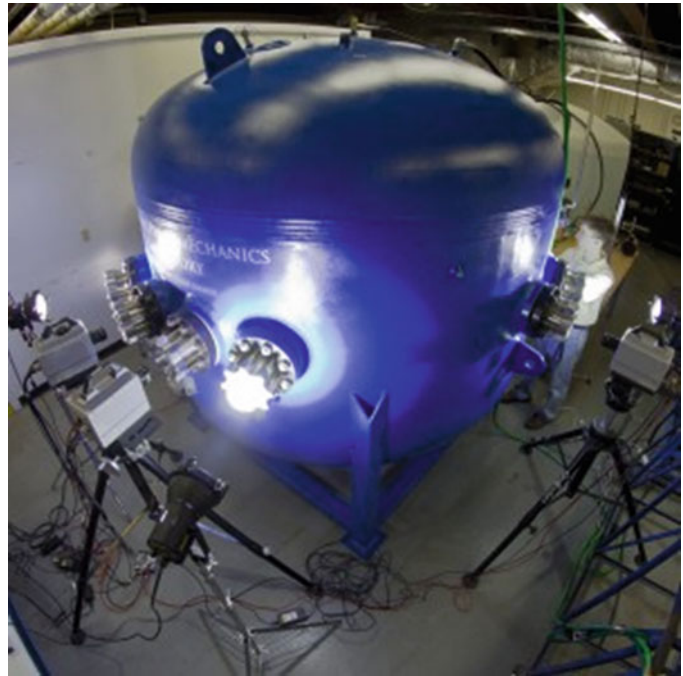
14.3 Experimental Methods

All implosion experiments are conducted in a large (2.1 m dia. \times 2.1 m height) pressure vessel with a maximum pressure rating of 6.89 MPa to simulate free-field conditions to monitor the evolution of pressure waves, and to provide constant hydrostatic pressure throughout the collapse event (see Fig. 14.1). Several Plexiglass windows mounted about the midspan of the pressure vessel allow the specimens to be viewed by cameras and adequately lit by two high powered light sources.

The specimens are sealed using two aluminum end caps, each inserted 12.7 mm into the tube, thereby reducing the unsupported length by 25.4 mm. The sealed tube is then suspended horizontally in the center of the pressure vessel using several steel cables attached to the inner walls of the vessel. A random speckle pattern is applied to a region spanning the entire length of the specimen and approximately half of the circumference using flat black paint. This region is painted white prior to speckling to enhance the contrast of the pattern. The tubes are secured in such a way that they cannot move or float during the filling process and the painted surface is faced toward the viewing windows. To measure the changes in local pressure during the collapse event, several high pressure blast transducers (PCB 138A05, PCB Piezotronics, Inc., Depew, NY) are mounted at different locations about the specimen both axially and circumferentially. The amplified outputs of these sensor are monitored by an Astro-med Dash[®] 8HF-HS portable data recorder (Astro-Med Inc., West Warwick, RI) at a sampling rate of 2 MHz.

The vessel is then flooded with water that is first filtered for maximum optical clarity, leaving a small air pocket at the top. Once the vessel is filled, nitrogen gas is introduced into the air pocket to pressurize the enclosed water. The pressure inside the vessel is increased at a gradual rate (83 kPa/min) until the specimen collapsed. At this point, the cameras and pressure sensors are end triggered to record the data occurring 1 s prior to triggering. In this way, data is collected for the entire collapse event by all recording devices. Post-mortem images are taken immediately after removal using a Nikon D90 DSLR camera to minimize potential creep.

Fig. 14.1 Pressure vessel used for implosion experiments



Two high-speed cameras (Photron SA1, Photron USA, Inc.), offset by 16° are used to capture stereo images of the patterned region of the specimen at 20,000 frames/s for glass/PE tubes, and 36,000 frames/s for carbon/epoxy tubes. The stereo images are analyzed using a commercially available digital image correlation (DIC) software, VIC3D 2012 (Correlated Solutions, Inc., Columbia, SC) to determine real-time, full-field displacements across the viewable surface of the specimen throughout the implosion event with a spacial resolution of 0.5 mm. The digital cameras have a resolution of $1,024 \times 1,024$ pixels. The lenses used for each experiment are selected as to image the entire width of the specimen throughout the collapse process, and to capture the full unsupported length of the cylinders.

14.4 Results

The glass/PE tubes imploded at a critical pressure of 2.03 MPa, while the carbon/epoxy tubes collapsed at a pressure of 1.61 MPa. These observed buckling pressures are reasonably close to the predictions made based on the methods of Rasheed [15] and Koudela [16]. Both specimen types collapsed completely in a mode 2 buckling shape, and regained some of their original circularity after pressure is removed.

Figure 14.2 shows typical pressure histories about the midspan of glass/PE tubes. This trace shows a fairly smooth drop in local pressure, followed by a sharp spike which decays gradually and is followed by many oscillations. This is consistent with previous work done by Turner [7] and Farhat [8] on metallic cylinders and shows that some of the same mechanisms are at play. The drop in pressure between points A and B are a result of the cylinder walls collapsing in toward each other. Surrounding fluid accelerates to follow the walls of the reducing cylindrical volume causing the local pressure to drop. This is confirmed by examining the images corresponding to points A and B in Fig. 14.3.

At point C, we see a rapid spike in pressure spike, taking approximately $300 \mu\text{s}$ rise from the minimum pressure to the maximum pressure. This spike corresponds to the walls of the cylinders contacting each other and arresting their movement, as seen in the matched image in Fig. 14.3. When the walls suddenly stop, so must the fluid accelerated during the previous stage of the collapse, and this rapid change in momentum results in the release of a pressure wave. Following the pressure spike at time C, the pressure drops back down to roughly hydrostatic as the buckled shape spreads axially along the cylinder, causing catastrophic damage to the specimen. In these images, a great deal of damage is clearly visible. The majority of this damage is in matrix cracking and delamination, manifesting in the “ribboning” seen in the high speed images. Upon further post-mortem investigation of the specimens, it is also clear that a good deal of fiber pull-out is present. These features are important to note, as they are energy intensive damage processes which affect the speed of the collapse and thereby the local pressure history.

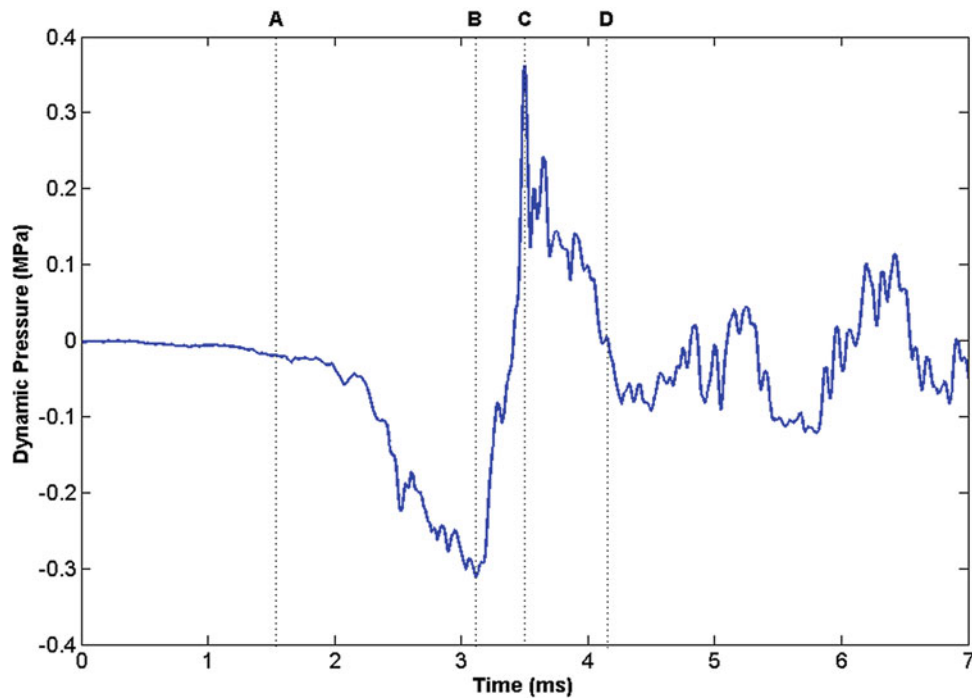


Fig. 14.2 Typical dynamic pressure trace about midspan of glass/PE tubes

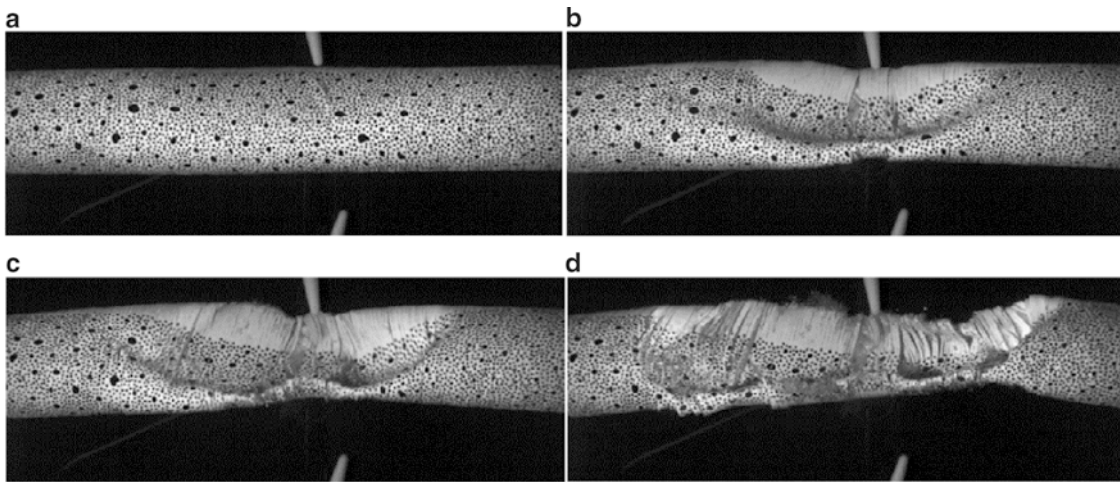


Fig. 14.3 High speed images of implosion event for glass/PE tube

Figure 14.4 shows a typical pressure history about the midspan of carbon/epoxy tubes. At first glance, the key points of this trace resemble that of the glass fiber tubes: the local pressure begins to drop gradually at point A and falls to a minimum at point B. The pressure then rises to a sharp peak at point C, followed by a broader region of lower overpressure until finally returning to hydrostatic pressure at point D.

However, we can notice two major differences in this pressure trace: a much more peaky underpressure region, and a much sharper and greater pressure spike. The small peaks in the underpressure region are due to localized catastrophic material failures coupled with the collapse of cavitation bubbles on the specimen surface. The collapse of these small bubbles release pressure pulses, adding some noise to the data in this region.

From the images in Fig. 14.5 we can see that from point A to point B, the structure deforms with very little visible damage. Similarly, the pressure trace this region shows a fairly smooth drop in local pressure. At point B, pressure is seen to drop suddenly as the first cracks appear along the length axis of the specimen. Between points B and C, through-thickness

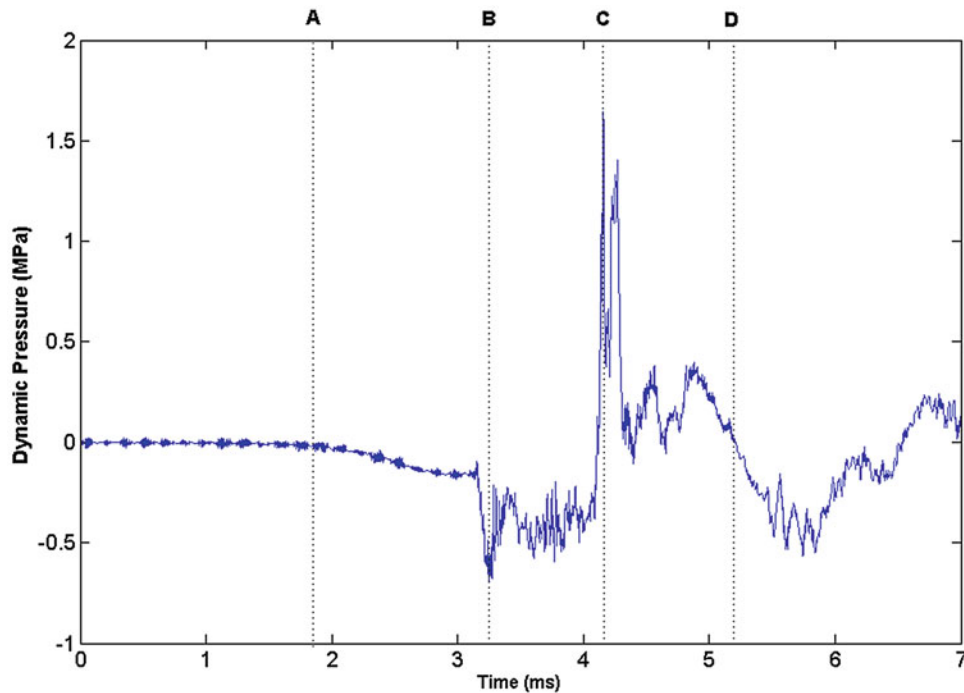


Fig. 14.4 Typical dynamic pressure trace about midspan of carbon/epoxy tubes

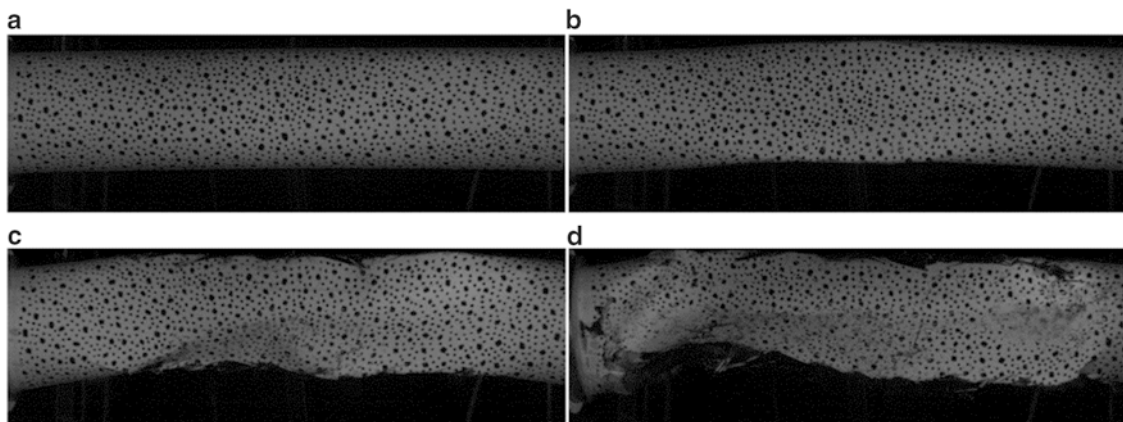


Fig. 14.5 High speed images of implosion event for carbon/epoxy tube

longitudinal cracks continue to progress very rapidly through the length of the specimen causing it to accelerate swiftly through the completion of collapse. After point C, the cylinder wall contact propagates through the length of the cylinder, resulting in the positive pressure region between C and D.

To compare these pressure traces more quantitatively, the minimum and maximum pressures are determined as a percentage of hydrostatic pressure, and the specific impulse of the under and overpressure regions are calculated. The specific impulse is defined as the area under the pressure curve for the time interval of interest. These quantities are compared in Fig. 14.6. Here it is found that carbon/epoxy tubes reach a lower minimum pressure, a higher maximum pressure, and deliver a much greater impulse in the pressure pulse emitted upon collapse.

The cause of this increase in pressure and impulse is a result of the increased speed of collapse observed in the high-speed imaging. Due to the catastrophic nature of the collapse of carbon/epoxy tubes, the specimens lose structural stability quite severely early in the implosion event, allowing them to fail at a higher rate. DIC is used to confirm and quantify this difference in collapse speed. The DIC system is first calibrated to collect accurate displacements on the surface of the submerged specimens. The accuracy is then confirmed for each specimen by comparing the outer radius of the specimen calculated by the software to its true value. A finite difference scheme is applied to the measured displacements to calculate

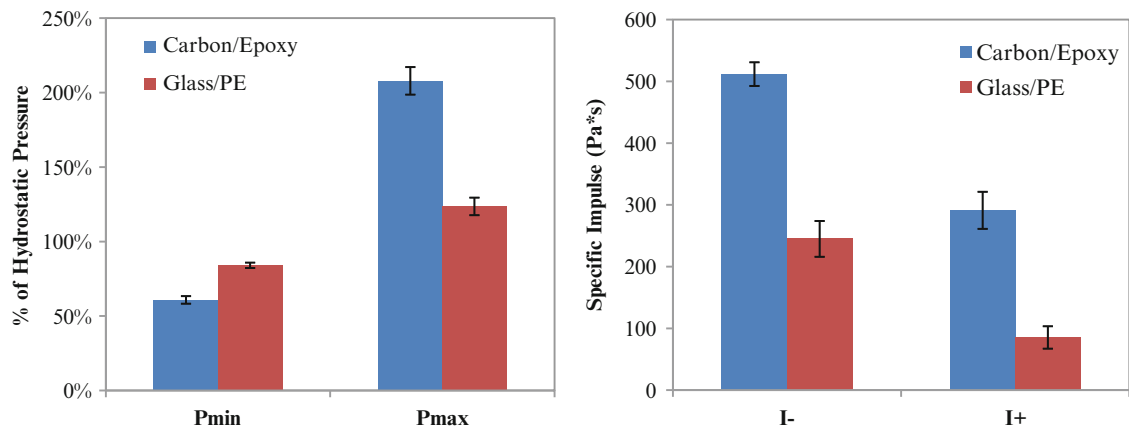


Fig. 14.6 Under/overpressure values (*left*) and calculated specific impulses (*right*) for different material systems

velocities of deformation. Collapse velocities are measured at the midspan of each specimen and the maximum values are used for comparison. Using this method, the initial velocities of the carbon/epoxy tubes are found to be significantly greater than those of glass/PE specimens, corroborating with previous observations.

Finite element analysis is performed using the commercially available ABAQUS software package (Dassault Systèmes Americas Corp., Waltham, MA) to confirm experimental observations and better understand the physics of the collapse process. Both linearized buckling analyses and non-linear Rik's method analyses are performed on the composite structures. For each type of specimen tested, these analyses accurately reproduce the observed critical collapse pressure and mode shapes of the implodable volumes, and aid in the understanding of the progression of their failure.

14.5 Conclusions

As a result of this study, the failure, damage progression, and pressure pulse released during the hydrostatic collapse of filament wound composite tubes is characterized. It is concluded that upon implosion, glass/PE filament wound tubes generate pressure waves with significantly reduced damage potential as compared with carbon/epoxy tubes of the same make. As seen in the collapse images, these tubes contain more energy intensive damage processes, such as delamination and fiber pull-out, causing less of the potential hydrostatic energy available to be transferred into the pressure pulse. The increased energy cost of deformation is also reflected in the speed of collapse, which for glass/PE tubes is roughly half that of carbon/epoxy tubes.

Another important finding is the difference between the negative impulse and positive impulse of the pressure history. In previous work by Turner [7] and Farhat [8], the negative and positive impulses of imploding glass and metallic volumes are found to be roughly equal. However in both carbon and glass fiber composites studied here, the positive impulse is significantly lower than the negative impulse. This shows that the complex damage and failure mechanisms present in both of these materials serve to dissipate much of the energy that would otherwise be released in the form of the pressure pulse. This in turn makes filament wound composite tubes a more attractive option when considering the potential of the material to damage nearby structures should an implosion occur.

Acknowledgements The authors kindly acknowledge the financial support provided by Dr. Yapa D. S. Rajapakse, under the Office of Naval Research (ONR) Grant No. N00014-10-1-0662, as well as Sachin Gupta, Craig Tilton, and Christopher Shillings for their invaluable help in conducting experiments.

References

1. Mouritz AP, Gellert E, Burchill P, Challis K (2001) Review of advanced composite structures for naval ships and submarines. *Compos Struct* 53(1):21–42
2. Accident grounds neutrino lab—physicsworld.com [WWW document], n.d. <http://physicsworld.com/cws/article/news/2001/nov/15/accident-grounds-neutrino-lab>. Accessed 2 Oct 2014

3. Ling J, Bishai M, Diwan M, Dolph J, Kettell S, Sexton K, Sharma R, Simos N, Stewart J, Tanaka H, Viren B, Arnold D, Tabor P, Turner S, Benson T, Wahl D, Wendt C, Hahn A, Kaducak M, Mantsch P, Sundaram SK (2013) Implosion chain reaction mitigation in underwater assemblies of photomultiplier tubes. *Nucl Instrum Methods Phys Res Sect A Accel Spectrometers Detect Assoc Equip* 729:491–499
4. Orr M, Schoenberg M (1976) Acoustic signatures from deep water implosions of spherical cavities. *J Acoust Soc Am* 59:1155–1159
5. Harben PE, Boro C (2001) Implosion source development and diego garcia reflections. Presented at the 23rd Department of Defense/Department of Energy Seismic Research Review, Jackson Hole, Wyoming
6. Turner SE (2007) Underwater implosion of glass spheres. *J Acoust Soc Am* 121:844–852
7. Turner SE (2012) Underwater implosion of cylindrical metal tubes. *J Appl Mech* 80(1):011013
8. Farhat C, Wang CG, Main A, Kyriakides S, Lee LH, Ravi-Chandar K, Belytschko T (2013) Dynamic implosion of underwater cylindrical shells: experiments and computations. *Int J Solids Struct* 50(19):2943–2961
9. Moon CJ, In-Hoon K, Bae-Hyeon C, Jin-Hwe K, Choi JH (2010) Buckling of filament-wound composite cylinders subjected to hydrostatic pressure for underwater vehicle applications. *Compos Struct* 92(9):2241–2251
10. Ross CTF, Little APF, Haidar Y, Waheeb AA (2011) Buckling of carbon/glass composite tubes under uniform external hydrostatic pressure. *Strain* 47:156–174
11. Smith PT, Ross CTF, Little APF (2009) Collapse of composite tubes under uniform external hydrostatic pressure. *J Phys Conf Ser* 181:156–157
12. Hernández-Moreno H, Douchin B, Collombet F, Choqueuse D, Davies P (2008) Influence of winding pattern on the mechanical behavior of filament wound composite cylinders under external pressure. *Compos Sci Technol* 68(3–4):1015–1024
13. Hur SH, Son HJ, Kweon JH, Choi JH (2008) Postbuckling of composite cylinders under external hydrostatic pressure. *Compos Struct* 86(1–3):114–124
14. Yang C, Pang SS, Zhao Y (1997) Buckling analysis of thick-walled composite pipe under external pressure. *J Compos Mater* 31(4):409–426
15. Rasheed HA, Yousif OH (2005) Stability of anisotropic laminated rings and long cylinders subjected to external hydrostatic pressure. *J Aerosp Eng* 18(3):129
16. Koudela KL, Strait LH (1993) Simplified methodology for prediction of critical buckling pressure for smooth-bore composite cylindrical shells. *J Reinf Plast Compos* 12(5):570–583